Available online at www.sciencedirect.com
SCIENCE DIRECT®
International Journal of Pharmaceutics 250 (2003) 13–23
international journal of pharmaceutics
www.elsevier.com/locate/ijpharm

Artificial neural networks (ANNs) and modeling of powder flow

K. Kachrimanis, V. Karamyan, S. Malamataris *

Department of Pharmaceutical Technology, School of Pharmacy, University of Thessaloniki, Thessaloniki 54124, Greece

Received 4 February 2002; accepted 30 July 2002

Abstract

Effects of micromeritic properties (bulk, tapped and particle density, particle size and shape) on the flow rate through circular orifices are investigated, for three pharmaceutical excipients (Lactose, Emcompress and Starch) separated in four sieve fractions, and are modeled with the help of artificial neural networks (ANNs). Eight variables were selected as inputs and correlated by applying the Spearman product-moment correlation matrix and the visual component planes of trained Self-Organizing Maps (SOMs). Back-propagation feed-forward ANN with six hidden units in a single hidden layer was selected for modeling experimental data and its predictions were compared with those of the flow equation proposed by Jones and Pilpel (1966). It was found that SOMs are efficient for the identification of co-linearity in the input variables and the ANN is superior to the flow equation since it does not require separate regression for each excipient and its predictive ability is higher. Besides the orifice diameter, most influential and important variable was the difference between tapped and bulk density. From the pruned ANN an approximate non-linear model was extracted, which describes powder flow rate in terms of the four network's input variables of the greatest predictive importance or saliency (difference between tapped and bulk density (x_2), orifice diameter (x_3), circle equivalent particle diameter (x_4) and particle density (x_8)):

$$W = b_0 + \{a_1[1 + \exp(b_2x_2 + b_3x_3 + b_4x_4 + b_8x_8)]^{-1} + a_2[1 + \exp(b'_3\chi_3 + b'_8x_8)]^{-1}\}.$$

Keywords: Artificial neural networks (ANNs); Powder flow rate; Self organizing maps (SOMs); Pharmaceutical excipients

1. Introduction

Flowability of powders is important for several processes involved in pharmaceutical formulation, such as storage, transfer, fluidization, blending, capsule filling and tableting.

Powder flowability depends on variables related to the material properties (particle size, shape, density, moisture content etc) or to the operator (equipment and handling, such as hopper width, wall angle, orifice diameter, storage time at rest and vibration before or during the flow). For the evaluation of powder flowability several methods

* Corresponding author. Tel.: +30-31-99-7651; fax: +30-31-99-7652
E-mail address: smalam@pharm.auth.gr (S. Malamataris).

0378-5173/02/$ - see front matter © 2002 Elsevier Science B.V. All rights reserved.
PII: S0378-5173(02)00528-8

have been used, either indirect (based on tapped density and angular properties) or direct (based on discharging rate through an orifice) by using more or less sophisticated equipment that can mimic the condition of real processing (de Greve et al., 1986). Since large number of variables may affect powder flow and for the description of these effects there are no simple relations based on first principles, the prediction of flow becomes difficult. For the pharmaceutical granulations an empirical, non-linear equation has been suggested by Jones and Pilpel (1966), which was derived from an earlier equation of Brown and Richards (1965). This equation directly relates the mass flow rate (W) with the diameter of the orifice (D_O) and the bulk density (ρ_b) of the powder, but indirectly with other important material and operator variables:

$$D_O = A\left(\frac{4W}{60\pi(\rho_b)\sqrt{g}}\right)^{1/n} \quad (1)$$

where g is the gravitational constant and A and n are coefficients. Eq. (1) has the drawback of comprising in two coefficients (A and n) the effects of many variables (material or operators) and, therefore, should not apply to powders of a wide particle size distribution and/or differing in particle shape characteristics.

Recent developments in artificial neural networks (ANNs) may provide a powerful tool for the analysis and description of non-linear systems, such as flow of powders (Bourquin et al., 1998a,b; Basheer and Hajmeer, 2000) and Self-Organizing Maps (SOMs) have been employed for the classification of powder flowability and prediction of weight variation of tablets (Antikainen et al., 2000).

In the present study, the effects of the micromeritic properties (bulk, tapped and particle density, particle size and shape) on the flow rate through circular orifices are investigated, for three common pharmaceutical excipients separated in four sieve fractions, and are modeled with the help of ANNs and SOMs. SOMs are employed as an alternative to the Spearman product-moment correlation matrix for correlating the input variables. Experimental data of flow rate are obtained with orifices of different diameter and modeled with the help of a back-propagation feed-forward ANN and flow rate predictions are compared with those of Eq. (1). Causal and predictive importance ('sensitivity' or 'saliency', respectively) of the input variables is evaluated (Tetko et al., 1996; Sarle, 2000) and an approximate non-linear model describing the powder flow rate is extracted from the pruned ANN.

2. Materials and methods

2.1. Materials

Dicalcium phosphate dihydrate (Emcompress, Edward Mendell, NY, USA), Lactose (Svenska Mjolkhscocher AB, Sweden) and Starch (Colorcon Ltd., Orpington, UK) were used after classification by sieving in four fractions: 90–125, 125–150, 150–180 and 180–250 μm.

2.2. Micromeritic properties of powders

Particle size and shape was characterized by an image analysis system (Quantimet 500, Leica, Cambridge, England). At least 300 particles were measured in four optical fields of samples dispersed in paraffin oil. Particle size was expressed as equivalent circle diameter (CED) and shape as aspect ratio (ratio of maximum to minimum Feret diameter), roundness ($\text{Perimeter}^2/4 \times \pi \times \text{Area} \times 1.064$) and convexity (ratio of projection perimeter to the perimeter of the circumscribed convex polygon). Particle density (ρ_p) was measured on an air comparison pycnometer (Beckman, Model 930) and loose bulk (ρ_b) and tapped (ρ_t) density in a 50 ml cylinder by using a J. Engelsmann volumeter, (Model JEL ST 2, Germany).

2.3. Flow rate measurement

A specially constructed flow meter was used. It consisted of a metallic frame supporting a horizontally rotating aluminum disc (2 mm thick, with circular orifices of different diameter), a metallic orifice-shutter operating by pulling a lever and a glass tube as hoper (35 cm long and 4 cm internal diameter) vertically mounted upon the metallic

disk. Rotating of the disk allowed quick change of the orifice and its justification in relation to the hopper. The apparatus consisted only of glass and metal and was earthed, in order to avoid electrostatic charging.

The flow-meter was operated manually (by pulling the lever of orifice shutter) and the powder was allowed to discharge directly upon an electronic balance (A&D Ltd., Japan) connected to a computer, through an RS232 serial communication interface, for monitoring the mass of discharged powder. Data were collected with the help of Windmill serial communication software (Windmill, UK) and transferred to MS EXCEL. Powder flow rate was estimated from the slope of mass versus time plots and expressed as g s^{-1}.

2.4. Data modeling

The Stuttgart Neural Network Simulator (SNNS, VER. 4.2 for WIN32) was employed and feed-forward back-propagation networks were applied for the modeling and prediction of the flow rate. Also, the flow equation (Eq. (1)) was fitted to the experimental data by regression analysis and its predictive ability compared with those of ANN models. All statistical computations were performed using the SPSS VER. 9 statistical software package (SPSS Inc. Chicago, IL, USA).

Eight variables were selected as inputs to the network: (1) bulk density, ρ_b, (2) difference between bulk and tapped densities, $\rho_t - \rho_b$, (3) orifice diameter, D_O, (4) particle size, CED, (5) aspect ratio, (6) roundness, (7) convexity and (8) particle density. The corresponding particle density represented the excipient nature, so that no categorical variables were included as inputs. The measured particle mean diameter (CED) was used instead of the nominal sieve size fraction, to improve correlation. The correlation matrix of the input variables was constructed based on the Spearman product-moment correlation and compared with the visual component planes in trained SOMs. They were obtained by using a public-domain program, the SOM toolbox (available for download at http://www.cis.hut.fi/projects/som-toolbox/), implemented using MATLAB code (Mathworks Inc., USA). Then, a feed-forward network that relies on the back-propagation of error algorithm was developed as equivalent to multivariate multiple non-linear regression (Sarle, 1994).

The experimental flow rate data comprised a $3 \times 4 \times 4$ full factorial design, replicated three times (144 experiments). The factors were excipient's nature (as particle density, at three levels), sieve fraction (as measured CED, at four levels) and diameter of the orifice (four levels).

2.4.1. Network training

Two advanced variants of back-propagation were employed, the resilient propagation (Rprop) and the Rprop with maximum-posterior approach (Rprop-MAP). The latter algorithm does not require a validation set, leaving more data points available for training and testing the network. The training set was representing the whole experimental region since it was based on statistical design (Wu et al., 1996). One third of the experimental data (48 measurements) was used for training and the remaining for validation and testing (48 measurements in each, from replicates). Networks of eight inputs and one output, containing from two to 18 hidden units in one, two and three layers were tested. Linear activation function was selected for input and output units and logistic sigmoid function for the hidden units. The input and output patterns were scaled in the interval [0, 1] with 10% headroom, where the sigmoid function operates in the more linear region (Murtoniemi et al., 1994). The 'early stopping' method was applied to check for possible network over-training (memorization of the noise, not just the signal, in the training patterns) and degradation of network performance. Training was stopped at 500, 1000, 3000, 5000 and 10 000 cycles and the correlation coefficient of the target flow rate values versus the network prediction was calculated as a measure of its predictive performance. After training, pruning (size reduction) was performed in order to simplify the neural network model, improve its generalizing ability and extract an approximate regression equation relating powder flow rate to the most important micromeritic properties. The Magnitude-Based Pruning algorithm was used, selected as the simplest pruning method (Seemann et al.,

1997). A 0.5% error increase and an error sum of square (SSE) of 0.004 were tolerated and training whilst pruning was performed for 100 cycles.

2.4.2. Ranking of input variables

Causal and predictive importance ('sensitivity' or 'saliency', respectively) of the input variables was evaluated in order to understand the underlying mechanisms of their effects on the powder flow. The modified link-weight-magnitude approach for non-linear relations was selected for the case of 'sensitivity' (Tetko et al., 1996). Regarding 'saliency' setting mean values of the inputs and retraining of the network was employed (Sarle, 2000).

3. Results and discussion

Micromeritic properties of the fractionated excipients that were considered as inputs of the ANN are listed in Tables 1 and Table 2 are summarized the experimental results of flow rate.

From Table 2 it can be seen that flow rate increases with the size of the orifice employed, as expected, and shows great variability between excipients. Also, the flow rate increases in general with the particle size increase, except of the larger particle size fraction of lactose (for all the orifices employed) and of Emcompress (for the smallest orifice of 0.5 cm). This flow rate decrease should be attributed to partial blocking of the orifice due to formation of more stable powder arches, while the variability between excipients should be related to micromeritic properties not considered in the experimental design, such as density (bulk, tapped and particle), particle shape and surface roughness.

3.1. Fitting of the flow equation

Predictive ability of flow equation (Eq. (1)) or of the modified version in which particle density replaced the bulk density (Jones and Pilpel, 1966) is summarized in Table 3, estimated by linear regression analysis of $\ln(4W/60\pi\rho_b\sqrt{g})$ or $\ln(4W/60\pi\rho_P\sqrt{g})$and $\ln(D_O)$. Results are given irrespective of particle size, for each diluent and for all the three diluents (using ρ_b or ρ_p). From Table 3 it is seen that fitting is relatively good for each diluent separately (high correlation coefficients), the predictive ability of Eq. (1) for flow rate is satisfactory (low values of PRESS) and the value of the exponent is very close to the theoretical ($n = 2.5$). Taking a closer look at the values of the regression parameters we can see that the predictive ability of Eq. (1) decreases in the order: Emcompress > Starch > Lactose. Comparing the regression parameters (Table 3) and the micromeritic properties (Table 1) we can see that for the

Table 1
Micromeritic properties of the fractionated excipients

Excipient	Sieve fraction (μm)	Density (g cm^{-3})		Particle diameter CED (μm)	Aspect ratio	Roundness	Convexity
		Bulk ρ_b	Tap-bulk $\rho_t-\rho_b$				
Emcompress	90–125	0.847	0.086	70	1.68	1.43	1.28
»	125–150	0.826	0.119	146	1.44	1.37	1.11
»	150–180	0.833	0.103	163	1.42	1.36	1.13
»	180–250	0.844	0.109	208	1.41	1.41	1.14
Lactose	90–125	0.842	0.119	22	2.11	1.57	1.29
»	125–150	0.737	0.074	115	1.62	1.33	1.20
»	150–180	0.727	0.078	145	1.46	1.36	0.12
»	180–250	0.712	0.061	223	1.45	1.32	1.13
Starch	90–125	0.646	0.109	85	1.50	1.31	1.09
»	125–150	0.658	0.103	116	1.51	1.27	1.07
»	150–180	0.674	0.100	138	1.47	1.29	1.08
»	180–250	0.663	0.090	215	1.52	1.34	1.10

Particle density was: 2.39 for emcompress, 1.54 for lactose and 1.50 (g cm^{-3}) for starch.

Table 2
Experimental results of flow rate measurement through circular orifices of different diameter

Sieve fraction (μm)	Orifice diameter (cm)	Flow rate of excipients (g s^{-1})		
		Emcompress (mean ± S.D.)	Lactose (mean ± S.D.)	Starch (mean ± S.D.)
90–125	1.8	45.1 ± 1.4	61.1 ± 1.6	27.5 ± 2.4
125–150	1.8	57.6 ± 2.4	230.7 ± 3.2	34.0 ± 2.9
150–180	1.8	57.3 ± 1.1	256.3 ± 2.7	42.2 ± 2.2
180–250	1.8	60.1 ± 1.7	236.7 ± 1.9	52.9 ± 4.9
90–125	1.5	31.5 ± 2.9	69.3 ± 2.0	20.4 ± 1.1
125–150	1.5	37.4 ± 1.1	124.7 ± 4.7	24.2 ± 2.4
150–180	1.5	39.4 ± 0.1	161.5 ± 2.0	26.3 ± 1.0
180–250	1.5	40.3 ± 0.3	152.8 ± 2.6	28.8 ± 2.5
90–125	1.0	10.8 ± 0.3	19.5 ± 1.9	7.2 ± 0.1
125–150	1.0	12.6 ± 0.1	54.0 ± 2.2	8.6 ± 0.1
150–180	1.0	12.7 ± 0.1	55.9 ± 0.6	9.2 ± 0.2
180–250	1.0	13.1 ± 0.2	54.0 ± 0.3	10.3 ± 0.1
90–125	0.5	1.87 ± 0.05	3.83 ± 0.29	1.20 ± 0.01
125–150	0.5	2.04 ± 0.01	8.97 ± 0.08	1.47 ± 0.01
150–180	0.5	2.01 ± 0.01	8.95 ± 0.24	1.54 ± 0.01
180–250	0.5	1.97 ± 0.01	8.02 ± 0.01	1.64 ± 0.01

different sieve fraction of Lactose, the micromeritic properties (especially the difference between tapped and bulk density ($\rho_b - \rho_t$) and aspect ratio) show the greatest variations, followed for those of Emcompress and Starch. Such variations should be the possible reason of the decrease in the predictive ability of Eq. (1), since only bulk and particle density were considered. Regression analysis for all the three diluents (combined data) gave lower correlation coefficient (0.867 and 0.842 when bulk or particle density is considered, respectively). This means low general applicability of Eq. (1) or existence of limitations concerning the particle density, size and shape. Therefore, different regression equations have to be used for different materials or even for the same material but for fractions of different particle size or shape. Thus the suggestion of a neural network model taking into account density, size and shape characteristics is justified.

3.2. Correlation of the input variables

Correlation of the micromeritic properties as input variables or screening of redundant inputs is presented in Table 4 as the Pearson product-moment correlation matrix and in Fig. 1 as component planes obtained with SOMs, in which

Table 3
Results of the linear regression analysis of $\ln(4W/60\pi\rho*\sqrt{g})$ vs. the logarithm of orifice diameter, $\ln(D_O)$

Regression summary	Emcompress	Lactose	Starch	Combined data	
				Using ρ_b	Using ρ_p
R	0.997	0.931	0.990	0.867	0.842
PRESS	0.050	1.150	0.180	5.990	7.000
R^2_{pred}	0.994	0.852	0.977	0.270	0.699
Intercept ($\ln A$)	0.013	−0.437	0.057	−0.092	0.156
Inverse slope (n)	2.634	2.932	2.597	3.419	3.624

Correlation coefficient (R), prediction error sum of squares (PRESS), prediction correlation coefficient (R^2_{pred}), and equation constants: intercept ($\ln A$) and inverse slope (n). $\rho*$, bulk density; ρ_b, differing for each size fraction or particle density; ρ_p, differing for each diluent.

similar color indicates homogeneous regions of similar values.

From Table 4, it can be seen that bulk density is correlated to particle density (correlation coefficient 0.80) and to roundness as well (correlation coefficient 0.75). Furthermore, roundness is correlated to aspect ratio (0.78) and aspect ratio is correlated to particle size (0.75). The correlation coefficients are relatively low (<0.95) and very similar and, therefore, none of the correlated variables could be omitted from the network. Also, from the component planes (Fig. 1) it can be seen clearly that bulk and particle density present the most similar patterns (high correlation), followed by roundness and aspect ratio. Some similarity is evident between bulk density and roundness, and between aspect ratio and particle size (CED). Consequently it is possible to rank the correlated variables on the basis of SOM similarity, though this cannot be expressed quantitatively. Comparing the correlation matrix (Table 4) with the more easily perceivable by the human brain visual presentation (Fig. 1), it is more clearly visible that no variable is correlated enough to be omitted from the network. Therefore, the visual inspection of SOMs is much more informative than the numerical matrix and seems to be advantageous justifying its use.

3.3. Artificial neural network modeling

The training and validation of networks, with different number of hidden layers and units, after 1500 cycles, employing the Rprop algorithm, is presented in Table 5 as mean square error (MSE). The limit of 1500 training cycles was selected because the validation error did not decrease substantially upon further training. From Table

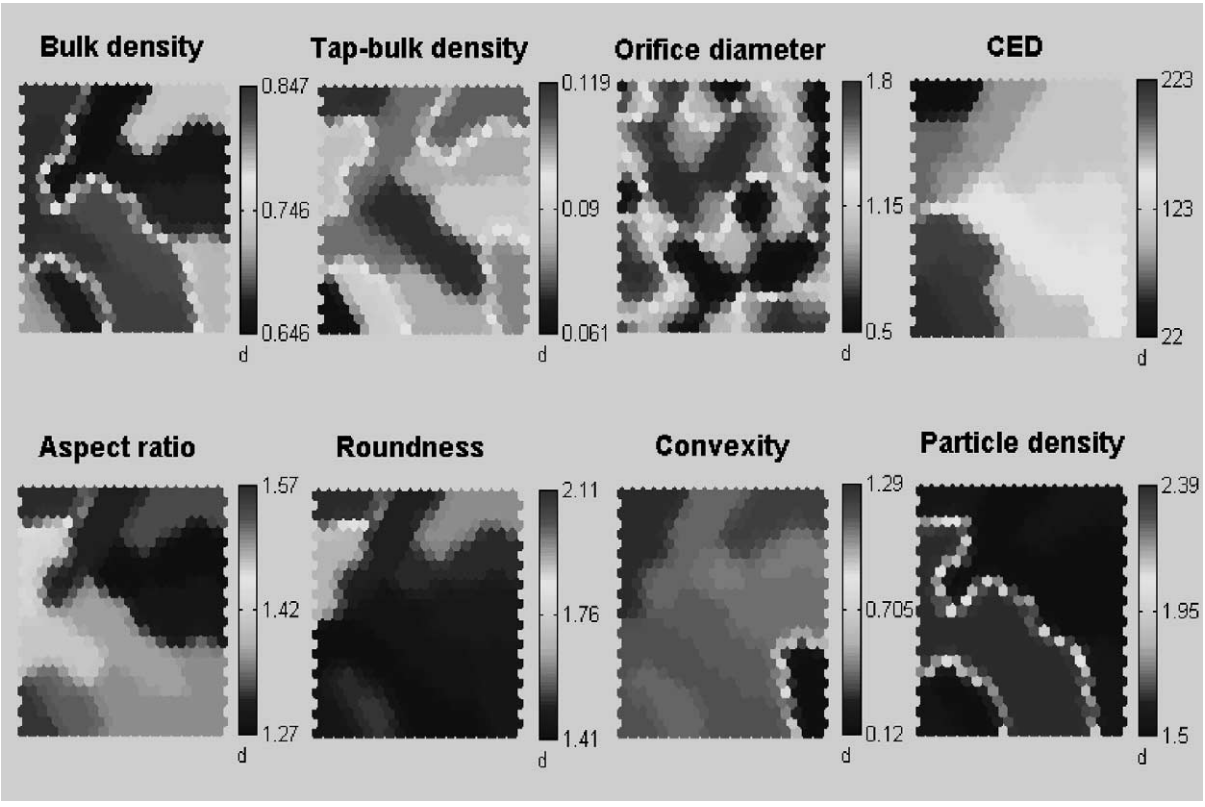

Fig. 1. Component planes of the input variables obtained with SOMs.

Table 4
Correlation matrix of the input variables

	ρ_b (g cm^{-3})	$\rho_t-\rho_b$ (g cm^{-3})	Orifice diameter (cm)	Particle diameter (μm)	Aspect ratio	Roundness	Convexity	Particle density (g cm^{-3})
ρ_b	1.00	0.30	0.00	−0.19	0.31	0.75	0.25	0.80
$\rho_t-\rho_b$	–	1.00	0.00	−0.37	0.22	0.34	0.28	0.32
Orifice size	–	–	1.00	0.00	0.00	0.00	0.00	0.00
Particle diameter	–	–	–	1.00	−0.75	−0.47	−0.18	0.11
Aspect ratio	–	–	–	–	1.00	0.78	0.33	−0.22
Roundness	–	–	–	–	–	1.00	0.21	0.29
Convexity	–	–	–	–	–	–	1.00	0.24
Particle density	–	–	–	–	–	–	–	1.00

ρ_b, Bulk density; $\rho_t-\rho_b$, tapped density.

5, a network with six hidden units in one layer (Fig. 2a) was chosen for further evaluation, since the addition of more hidden layers does not seem to improve the network's performance. The network was also trained with the RpropMAP algorithm and its predictive ability (correlation coefficient, R, of the target flow rate values vs. the network prediction) was compared with that of the Rprop algorithm, after increasing number of training cycles. The results are listed in Table 6.

From the R values, Table 6, it can be seen that both training algorithms perform equally well and comparison to those corresponding to the predictive ability of the flow equation shows that the performance of the selected neural network model is better than that of Eq. (1). Furthermore, the network is not over-trained even after several thousands training cycles. On the contrary, its predictive ability improves, at least up to 10 000 training cycles (Table 6). Taking into account the rather small size of the training set (48 data points), over-training of the network is possible, but as we can see from Table 2 the flow rate standard deviation is very small (<5 g s^{-1} or relative S.D. $<10\%$) and, therefore, there is very little noise in the data and nothing to over-train. Also, the structures of the training set and the test set are similar, since they are replications of the same factorial design. All the above combined with the small network size consist good reasons for absence of over-training of the neural network model even after 10 000 training cycles.

The developed neural network model has the additional advantage over Eq. (1), that it can be used for flow rate prediction of all three excipients employed, since a parameter representing excipient type quantitatively (particle density) is used as input variable. In the contrary Eq. (1) requires a separate regression model for each excipient. Taking into account that the neural network utilizes only part of the total available data for training, and that it is not sensitive to over-training even after long training, it can be concluded that it is superior to Eq. (1) from more than one viewpoint. The superiority of the neural network model is attributed to its complex non-linear structure, since feed-forward back-propagation networks are

Table 5
Mean square error (MSE) of training and validation for networks with eight inputs, one output and different number of hidden layers and units in each layer, after 1500 training cycles with the Rprop algorithm

Hidden layers	Units in each layer	Mean square error ($MSE \times 10^4$) of	
		Training	Validation
1	2	2.27	27.7
1	4	1.43	27.5
1	6	1.21	27.3
1	8	1.75	28.6
1	10	1.30	27.3
1	12	1.24	28.1
1	14	1.50	27.3
1	16	1.49	26.8
1	18	0.86	28.1
2	6	1.45	26.8
3	6	1.01	27.0

equivalent to multiple non-linear regression models.

3.4. Importance of input variables

The calculated values for causal importance (sensitivity) and predictive importance (saliency) of the input variable are presented in Table 7. Causal importance refers to the change of the output corresponding to a given change in an input variable, while predictive importance refers to the increase in the error function when an input is omitted from the network (Sarle, 2000). From Table 7 it can be seen that the values of sensitivity and saliency do not coincide and show that the difference between tapped and bulk density ($\rho_t - \rho_b$) is the most influential variable, closely followed by orifice diameter. Particle density and aspect ratio come next in sensitivity, while the rest of the variables are of minor importance. Regarding the predictive importance (saliency), orifice diameter is by far the most important variable, followed by the difference between tapped and bulk density, the particle density and the size. The rest of the variables play no important role in prediction and could be omitted from the network.

3.5. Extraction of approximate non-linear model

Taking into account the importance evaluation of the input variables (sensitivity and saliency), four hidden units were removed from the network and three inputs (bulk density, orifice diameter and particle density) were connected to both the remaining. The topology of the trained neural network after pruning by the Magnitude-Based algorithm is depicted in Fig. 2(b). The correlation coefficient of the predicted by the network values versus the target flow rate values was 0.980 for the pruned version. This shows that the ANN model preserved its predictive performance, while it was greatly simplified by removing unnecessary units and links.

From the pruned neural network, it is easier to extract an approximate model for the description of powder flow rate in terms of the network's input variables. Considering that the input and output layers use the linear activation function, while the hidden layer uses the sigmoid activation function, the equation expressing the initial ANN model before pruning (Fig. 2a) can be written as follows:

$$W = b_0 + \sum_{i=1}^{6} a_i \left[1 + \exp\left(\sum_{j=1}^{8} b_{ij} x_j\right)\right]^{-1} \quad (2)$$

where W is the output node (flow rate), x_j are the input variables, α_i represents the weights relating the six hidden nodes to the output node, and b_{ij} represents the weights relating the eight input nodes to the six hidden nodes. Then, taking into account only the four variables with the greatest saliency (tapped-bulk density, x_2, orifice diameter, x_3, particle diameter, x_4, and particle density, x_8) and the pruned links between inputs and hidden units, the Eq. (2) model can be refined as follows:

$$\begin{aligned} W = {} & b_0 \\ & + \{a_1[1 + \exp(b_2 x_2 + b_3 x_3 + b_4 x_4 + b_8 x_8)]^{-1} \\ & + a_2[1 + \exp(b'_3 \chi_3 + b'_8 x_8)]^{-1}\} \end{aligned} \quad (3)$$

which is an approximate non-linear model that can be fitted to the flow rate data of all excipients by multiple non-linear regression.

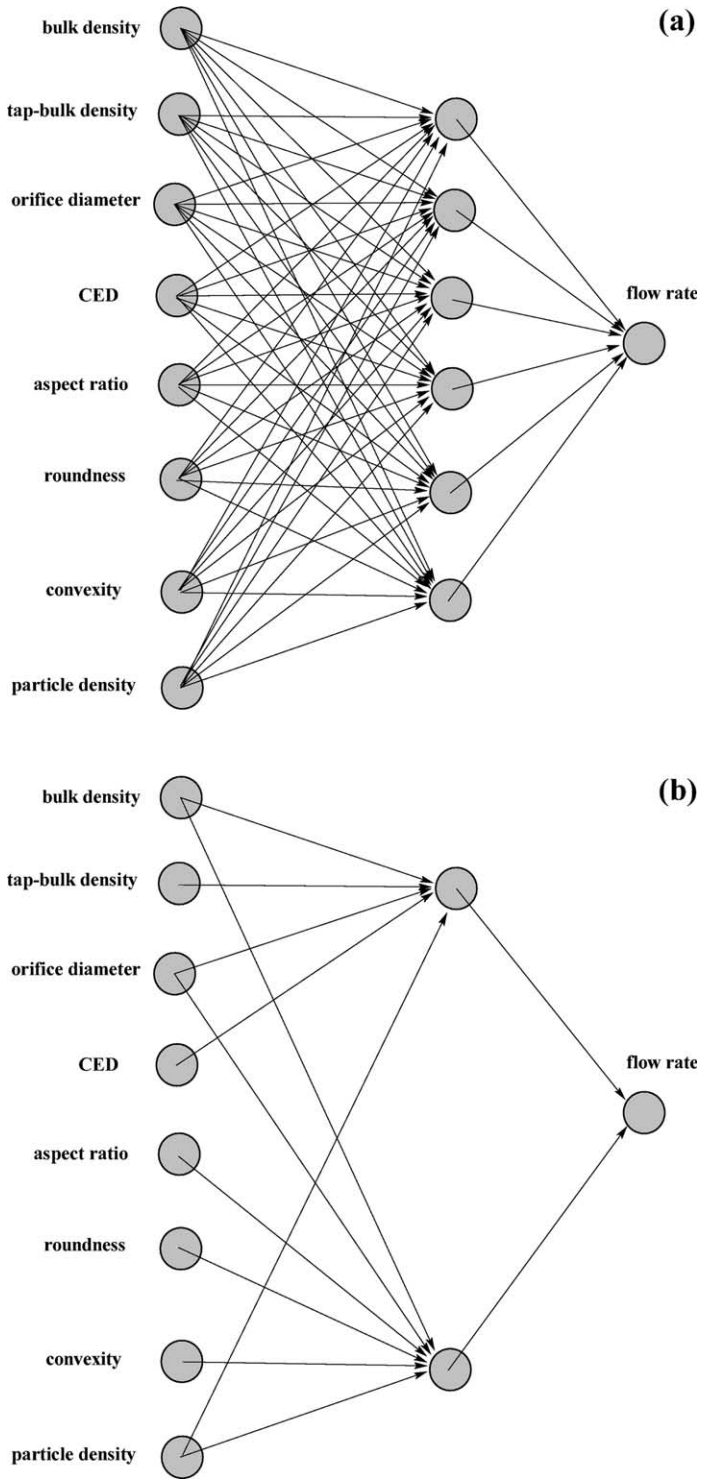

Fig. 2. Topology of the trained neural networks, (a) before and (b) after the pruning by the magnitude-based algorithm.

Table 6
Predictive performance (correlation coefficient, R, of the target flow rate values vs. the network prediction) of the selected ANN, (single hidden layer of six units, Fig. 2a), after increasing training cycles, using the Rprop and RpropMAP algorithms

Training cycles	Correlation coefficient (R), using algorithm	
	Rprop	RpropMAP
500	0.973	0.972
1000	0.976	0.981
3000	0.980	0.972
5000	0.986	0.989
10 000	0.993	0.992

Table 7
Causal importance ('sensitivity') and predictive importance ('saliency') of the input variables

Input variable	Sensitivity ($\times 10^3$)	Saliency ($\times 10^3$)
Bulk density (ρ_b)	148.55	0.19
Tap-bulk density ($\rho_t - \rho_b$)	1020.39	1.83
Orifice diameter	971.23	21.40
Particle diameter	180.26	0.64
Aspect ratio	244.72	0.11
Roundness	50.50	0.08
Convexity	116.35	0.10
Particle density	438.34	0.89

4. Conclusions

The suggested ANN model is superior to the flow equation (Eq. (1)), since its predictive ability is higher and does not require separate regression for each excipient. Besides the orifice diameter, most influential and predictive variable is the difference between tapped and bulk density ($\rho_t - \rho_b$) and the SOM networks have been efficient tools for the evaluation of input variables and identification of their co-linearity. Taking into account the four variables with the greatest predictive importance or saliency (tapped-bulk density (x_2), orifice diameter (x_3), circle equivalent particle diameter (x_4) and particle density (x_8)), an approximate non-linear model has been extracted:

$$W = b_0 + \{a_1[1 + \exp(b_2x_2 + b_3x_3 + b_4x_4 + b_8x_8)]^{-1} + a_2[1 + \exp(b'_3\chi_3 + b'_8x_8)]^{-1}\}$$

Acknowledgements

This work has been supported by the Tempus program JEP-10310-97 that enabled the study visit of V. Karamyan (Pharmacy post-graduate student from the State Medical University of ARMENIA).

References

Antikainen, O.K., Rantanen, J.T., Yliruusi, J.K., 2000. Use of the Kohonen self-organizing map to predict the flowability of powders. STP Pharm. Sci. 10, 349–354.

Basheer, I.A., Hajmeer, M., 2000. Artificial neural networks: fundamentals, computing, design, and application. J. Microbiol. Methods 43, 3–31.

Bourquin, J., Schmidli, H., van Hoogevest, P., Leuenberger, H., 1998. Advantages of Artificial Neural Networks (ANNs) as alternative modeling technique for data sets showing non-linear relationships using data from a galenical study on a solid dosage form. Eur. J. Pharm. Sci. 7, 5–16.

Bourquin, J., Schmidli, H., van Hoogevest, P., Leuenberger, H., 1998. Pitfalls of Artificial Neural Networks (ANN) modeling technique for data sets containing outlier measurements using a study on mixture properties of a direct compressed dosage form. Eur. J. Pharm. Sci. 7, 17–28.

Brown, R.L., Richards, J.C., 1965. Kinematics of the flow of dry powders and bulk solids. Rheol. Acta 4, 153–165.

de Greve, C., van Aerde, P., van Severen, R., 1986. Determination of flowability of pharmaceutical powders using a computerized strain gauge balance. Acta Pharm. Technol. 32, 63–66.

Jones, T., Pilpel, N., 1966. The flow properties of granular magnesia. J. Pharm. Pharmacol. 18, 81–93.

Murtoniemi, E., Yliruusi, J., Kinnunen, P., Merkku, P., Leiviskä, K., 1994. The advantages by the use of neural networks in modelling the fluidised bed granulation process. Int. J. Pharm. 108, 155–164.

Sarle, W., 1994. Neural networks and statistical models. Proceedings of the 19th Annual SAS Users Group International Conference, pp. 1–13.

Sarle, W., 2000. How to Measure the Importance of Inputs (ftp://ftp.sas.com/pub/neural/FAQ2.html#A_import). SAS Institute, Cary, NC, USA.

Seemann, J., Rapp, F.-R., Zell, A., Gauglitz, G., 1997. Classical and modern algorithms for the evaluation of data from sensor-arrays. Fresenius J. Anal. Chem. 359, 100–106.

Tetko, I., Villa, A., Livingstone, D., 1996. Neural network studies. 2. Variable selection. J. Chem. Inf. Comput. Sci. 36, 794–803.

Wu, W., Walczak, B., Massart, D.L., Heuerding, S., Erni, F., Last, I.R., Prebble, K.A., 1996. Artificial neural networks in classification of NIR spectral data: design of the training set. Chemom. Intell. Lab. Syst. 33, 35–46.